Three mirror cavities as an alternative for the production of frequency dependent squeezed light

Pedro Rodríguez
Mentors: Samuel Deleglise, Pierre Cohadon

July 2021

Abstract

One of the biggest issues that affects the detection of Gravitational Waves is the Quantum Noise (QN) caused due to the Heisenberg uncertainty being present in the nature of light. The current techniques to overcome this problem make use of non-linear crystals and Fabry-Perot (FP) cavities to produce squeezed light states and reduce the QN below the so called Standard Quantum Limit. The main problem is this works well just for certain frequencies of the laser since the QN is frequency dependent while the current squeezed light states are not. Just one state of squeezed light is not sufficient to achieve the optimum QN reduction for each frequency and hence the need for frequency dependent squeezed light. The reason why there is no frequency dependent squeezed light around is because FP cavities are not able to tune the bandwidths of their resonant peaks. Nonetheless, there is an alternative and it is to use Three Mirror (TM) cavities. This report shows how to derive the equations that govern TM cavities through a matrix formalism and shows that it is possible to reinterpret a TM cavity as being equivalent to an FP cavity with a tunable mirror. It is also shown that TM cavities are able to tune the bandwidths of their peaks by just adjusting the length of their first cavity between a range of half the wavelength of the resonance frequency of the cavity. Therefore, showing that in theory TM cavities are able to produce frequency dependent squeezed light.

Contents

1 Introduction

Currently, one of the biggest limitations towards better strain sensitivity within the Gravitational Waves (GW) detection is a type of noise called the Quantum Noise (QN). It is originated from the quantum nature of light itself where the amplitude and phase quadratures form a pair of conjugate observables [1]. The uncertainty in these two observables will bring to life two different noises, which sum equals the QN. These two noises are known as the radiation pressure noise (RPN) and the shot noise (SN) and the relation between the three noises is expressed as

$$QN = RPN + SN.$$

More intuitively, the RPN is caused due to the random fluctuations in the amplitude of the electric field, that translate into a fluctuating force acting on the interferometer mirrors due to radiation pressure. This fluctuating force, proportional to the laser power, translates into random mirror displacements, following the frequency dependence of the mirror mechanical susceptibility. Well above the resonance frequency of the mirror suspension, the amplitude of the RPN thus scales as $1/\Omega^2$. On the other hand, the SN is caused due to the random fluctuations in the phase of the electric field, which is translated into a photon error counting within the GW detectors. This noise is inversely proportional to the power of the laser but in its nature is not frequency dependent. The behaviors of the three noises can be seen in fig. 1. For each frequency Ω, there is a single laser power for which the contribution of SN and RPN are equal. One can show that this laser power is the one that minimizes the total QN. The corresponding sensitivity, called the Standard Quantum Limit (SQL), is the optimal sensitivity achievable at the frequency Ω with classical light. The locus of the SQL as a function of frequency is represented as a black dashed line in Fig. 1. At the particular laser power for which the SN (blue curve) and RPN (red curve) have been plotted, the SQL is only reached at around $\Omega/2\pi = 50$ Hz.

On the other hand, the SQL sensitivity can be exceeded by using so-called squeezed states of light. In such a state, the phase and amplitude variables of the field feature non-classical correlations, such that the noise is reduced in one quadrature, and increased in the conjugate quadrature. This technique, currently in use in the last generation of gravitational wave interferometers, exploits a non-linear crystal to generate a frequency-indepedent squeezed state. In LIGO and Virgo, the phase squeezing that is currently implemented allows one to reduce the detrimental impact of SN at high-frequency. A single squeezed state is however insufficient to beat the SQL over a large frequency span: indeed, at low frequency, RPN is the dominant noise, such that amplitude squeezing should be used in this frequency band while phase squeezing should be used at high frequency.

The role of a rotation cavity is precisely to achieve this frequency-dependent rotation of the squeezing. The idea is to generate a frequency-independent

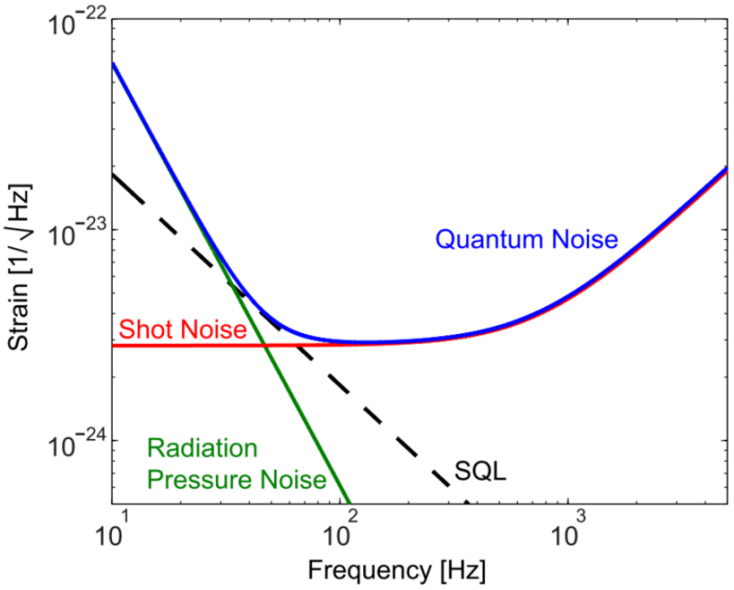

Figure 1: Plots of the QN, RPN and SN for classical light taken from [2]. Here the frequency dependencies of the noises can be seen.

squeezed-state with a non-linear crystal and to use the response of a Fabry-Perot cavity to rotate the quadratures of the field in a frequency-dependent manner. Since the typical corner frequency over which this rotation should occur is on the order of 100 Hz, the rotation cavity should have an extremely narrow bandwidth, which requires a cavity that combines a very long length and a high finesse. In the current design, the length of the rotation cavity is planned to be 300 m. A feature that would be highly desirable with such a rotation cavity would be the ability to tune the bandwidth in-situ, such that the corner-frequency could be quickly adjusted, for instance to match the corner frequency required for a given laser power. However, adjusting the bandwidth of a Fabry-Perot cavity usually requires to change the transmission of its mirrors, a process that is lengthy and requires a physical intervention on the setup.

This International Research Experience (IREU) research focused on the exploration of the ability of a Three mirror (TM) cavity being able to produce frequency dependent squeezed light. In the following, the reader will find a discussion on the essential bits of knowledge that need to be known to understand the workings of an FP cavity (section 2). Then, section 3 discusses the mathematical formalism used to develop the equations that govern the TM cavity, a proof that the TM cavity can be reinterpreted as an FP cavity with an effective mirror and the behavior that this cavity exhibits. The report finalizes by showing that indeed it is possible to tune the bandwidth of the cavity.

2 Fabry-Perot cavity

The following, is a discussion of the components, structure, functionality and characteristics of an FP cavity, how they relate to the physical properties of the mirrors composing it and some details of the current limitations of the FP cavity that were not mentioned in the introduction.

2.1 Basic components and structure

FP cavities are made-up of only two optical components which are free space and spherical mirrors. It is important to mention that even though spherical mirrors are preferred due to their surface being able to perpendicularly match at all points of the wave front of Gaussian beams, for the sake of simplicity, this reports presents an analysis done with plane lossless mirrors and plane waves. A simplified scheme of a plane mirror and free space components along with their parameters of interest and system of equations can be found in fig. 2. There, the variables a_{in}, a_{out}, b_{in} and b_{out} represent the complex amplitudes of ingoing and outgoing fields and the system of equations show how the outgoing amplitudes are modified by its respective optical component. This applies to both of the components in the figure.

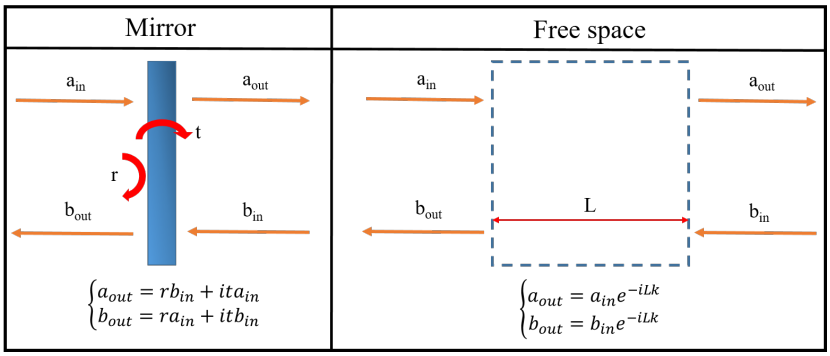

Figure 2: (On the left) Scheme of the mirror component, r and t represent the reflection and transmission coefficients. (On the right) Scheme of the free space component where L is the width of the component. The variables in both diagrams represent the amplitudes of the ingoing and outgoing light fields.

The r and t letters in the mirror scheme (and throughout the whole text) represent the reflectivity and transmission coefficients of the mirror. Both of them are real and positive numbers between 0 and 1. Except in section 3.4 where another convention is used to show the equivalence of the effective mirror model and the TM cavity. They determine how much of the ingoing light will be reflected (r coefficient) and how much of it will be transmitted (t coefficient). To get a better grasp of what these coefficient mean, if it is assumed that $b_{in} = 0$,

it is obtained that

$$r = \frac{b_{\text{out}}}{a_{\text{in}}} \quad \text{and} \quad t = \frac{a_{\text{out}}}{a_{\text{in}}}.$$

Then, since the square of the amplitude is the power of the light field, r and t can be related to the percentage of reflected power R and the percentage of transmitted power T by taking the division between the modulus square of the respective amplitudes. That is

$$r^2 = \frac{\|b_{\text{out}}\|^2}{\|a_{\text{in}}\|^2} = R \quad \text{and} \quad t^2 = \frac{\|a_{\text{out}}\|^2}{\|a_{\text{in}}\|^2} = T.$$

Bear in mind that these four quantities (r, t, R, T) are unitless. Finally, by the law of conservation of energy a lossless mirror can be defined as a mirror for which $T + R = 1$ implying that

$$r^2 + t^2 = 1$$

Now, the modifications done by the mirror component to the amplitude of the light is governed by the system of equations

$$\begin{cases} a_{\text{out}} = r b_{\text{in}} + i t a_{\text{in}} \\ b_{\text{out}} = r a_{\text{in}} + i t b_{\text{in}} \end{cases} \tag{1}$$

which is more or less intuitive except for the appearance of complex number i. It is placed there to ensure the unitarity of the transformation between input and output fields without breaking the symmetry between the equations.

The free space component, which also appears in fig. 2, is simpler to understand. In this case, the light amplitude modifications are dominated by the (well known) equations of light propagation in free space given by

$$\begin{cases} a_{\text{out}} = a_{\text{in}} e^{-iLk} \\ b_{\text{out}} = b_{\text{in}} e^{-iLk} \end{cases} \tag{2}$$

where L is just the length of the free space component and $k = \omega/c$ is the wave vector, where ω is the angular frequency of light and c the speed of light in free space.

Having met the central components, the structure of the cavity is now introduced as a system composed of two parallel mirrors with a vacuum in between them. This is depicted in fig. 3. The vacuum that happens to be in between the two mirrors is precisely the free space component and therefore the distance between the two mirrors is its L parameter. As it will be shown in the next section, it is this parameter which determines which frequencies will be resonant within the cavity and it is the t's of the mirrors which determine the bandwidth of the cavity. In the diagram of fig. 3, mirror 2 is missing one ingoing light amplitude in the bottom right since in practice the FP cavities for GW detectors only receive inputs from one side.

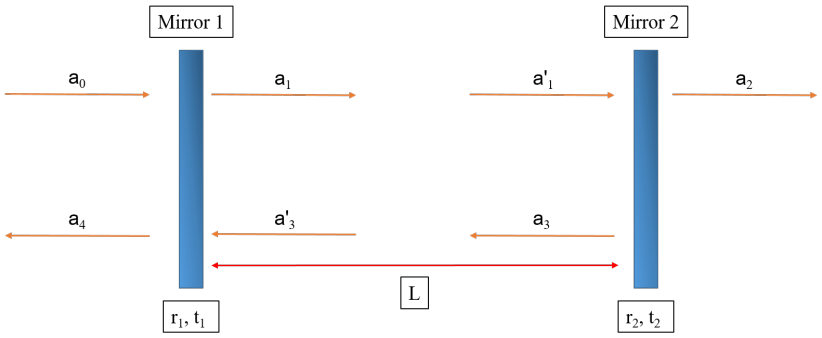

Figure 3: Simplified scheme of an FP cavity where L is the distance between the two mirrors and r_i and t_i are the reflection and transmission coefficients of the i^{th} mirror .

2.2 Functionality and characteristics

FP cavities are ubiquitous for the GW interferometers, where they can be used as spatial and frequency filters for the laser beam. By accumulating the position-dependent dephasing over several round-trips, optical cavities are used to boost the sensitivity of the detectors compared to a standard Michelson interferometer. Furthermore, these cavities function as optical systems that can store light of a particular wavelength between the two parallel mirrors. This functionality is quantified as the intracavity intensity dependent of the light frequency. The upper plot of fig. 4 shows how this looks for different hypothetical FP cavities all with $L = 5$m, different $T_1 = 0.02, 0.09, 0.3$ and each of the them have the same $T_2 = 0.001$. This same figure shows what are known as the resonance peaks which center occurs at every frequency of resonance $f_{\text{res}}=Nc/2L$ where N is just a positive integer.

The FP cavities can also manage to modify the phases (relative to the incoming beam) of their reflected and transmitted light fields. A property very much needed for the phase squeezing technique. The bottom plot in fig. 4 shows how the transmitted light field exhibits this change of phase. Notice that for the three cases that appear in the graph a change of approximately 0 degrees always occurs at the frequency of resonance. At the same time, notice that the bandwidth over which the phase shift occurs is given by the width of the resonance peak. This broadness of the peaks is quantified by the Full Width at Half Maximum (FWHM) which is two times the Bandwidth of the peaks. All of this is of no coincidence and this frequency-dependent rotation of the phase is precisely what is exploited in filter cavities to develop a frequency-dependent squeezing. Now, a list of several characteristics related to the workings of the cavity is presented:

- Round-trip time [τ]: The time it takes the light to do one round-trip

within the cavity.

$$\tau = \frac{2L}{c}$$

- Free Spectral Range [FSR]: The constant frequency spacing between two subsequent peaks of resonance.

$$FSR = \frac{c}{2L}$$

- Full Width at Half Maximum [FWHM]: The width of the peak at half its maximum value.

$$FWHM = \frac{2FSR}{\pi} \arcsin\left(\frac{1 - r_1 r_2}{2\sqrt{r_1 r_2}}\right) \approx \frac{FSR}{2\pi}(T_1 + T_2)$$

- Finesse [$\mathcal{F}$]: The average number of round trips undergone by light within the cavity before escaping through one of the mirrors.

$$\mathcal{F} = \frac{FSR}{FWHM} \approx \frac{\pi}{1 - r_1 r_2} \approx \frac{2\pi}{T_1 + T_2}$$

- Lifetime [τ_{cav}]: The time needed for the energy stored in the cavity to decrease by a factor of 1/e. It is also the typical response time of the intracavity field to a modification of the input fields.

$$\tau_{\text{cav}} = \mathcal{F}\tau$$

- Bandwidth [BW]: Half the FWHM and it is also the inverse of the τ_{cav}.

$$BW = \frac{FWHM}{2} \approx \frac{c}{8\pi L}(T_1 + T_2) = \frac{1}{\tau_{\text{cav}}} \tag{3}$$

As a final important characteristic of the cavity, the transmission and reflection coefficients of the cavity as a whole can be written as

$$t_{FP} = \frac{a_2}{a_0} = -\frac{t_1 t_2 e^{-iL_1 k}}{1 - r_1 r_2 e^{-2iL_1 k}} \tag{4}$$

$$r_{FP} = \frac{a_4}{a_0} = \frac{r_1 - r_2 e^{-2iL_1 k}}{1 - r_1 r_2 e^{-2iL_1 k}}. \tag{5}$$

3 Three mirror cavity

In this section it is presented how by using a matrix formalism we derived the reflection and transmission functions for the TM cavity. Then, we provide a proof that the three mirror cavity system would be equivalent to a two mirror cavity system with one of its mirror being an effective mirror (fig. 5).

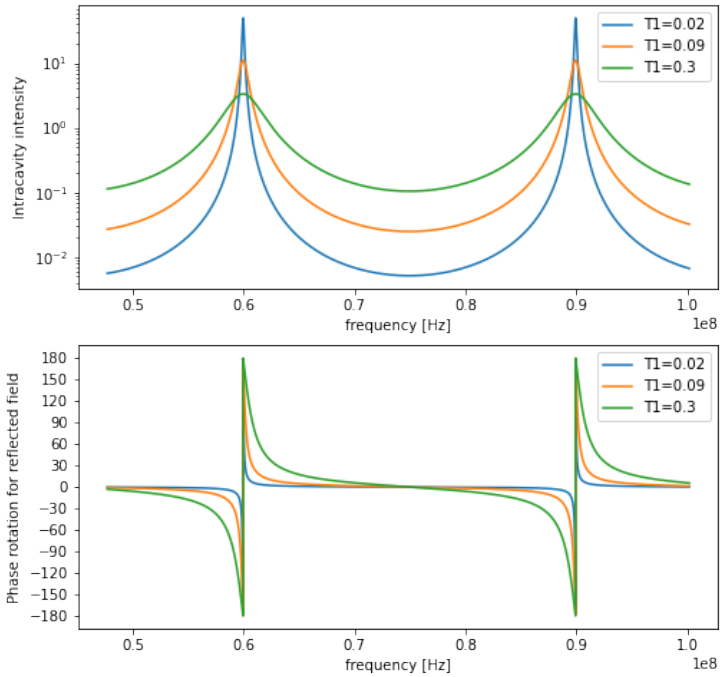

Figure 4: (upper plot) Intracavity intensity per light frequency.(bottom plot) The phase rotation per light frequency of the reflected field. The plots were made for three different hypothetical FP cavities all with $L = 5$m, the same $T_2 = 0.001$ for all the cavities and the T_1's are specified in the plot for each cavity.

3.1 The proposed solution

As it was mentioned in the introduction, the problem with the current FP cavities is their inability of changing the transmission coefficients of its mirrors. Nonetheless, notice that if one imagines the FP cavity system as one sole effective mirror, then the transmission and reflection coefficients (defined as t_{eff} and r_{eff}) of this effective mirror would be equivalent to the equations (17) and (18) respectively. Allowing the tunability of t_{eff} by just adjusting the distance between the mirrors of the FP cavity. Then, the goal is to use this effective mirror along with a normal mirror to create an FP cavity with a tunable bandwidth. In other words, this would be a three mirror cavity with two of its mirrors very close together, such scheme appears in fig. 5. Therefore, to understand the

viability of using a TM cavity to produce frequency dependent squeezed light its transmission and reflection coefficients (defined as t_{TM} and r_{TM}) are derived in the following sections.

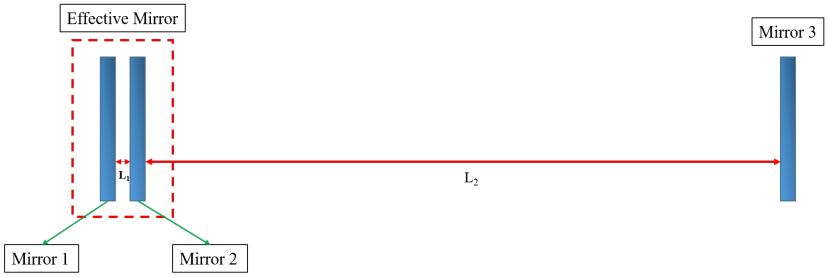

Figure 5: Scheme representing how by using a TM cavity one could create an FP cavity with a tunable bandwidth. Here L_1 and L_2 represents the distances between the mirrors. Notice that the trick lies in making $L_1 \ll L_2$

3.2 Matrix formalism

To obtain the equations that govern the reflection and transmission functions of the three mirror cavity the matrix formalism that appears (in more detail) in ref. [1] was used. To understand this technique let us build from the bottom to the top. As it was previously discussed mirrors and free space are optical components that receive input light fields and produce output light fields modified according to their system of equations. Then, these system of equations can be rearranged in such a way as to obtain a matrix equation that receives as an input the light fields that are in one side of the component and produces as an output the light fields that are on the other side of the component. For the mirror this matrix equation would look like

$$\begin{bmatrix} a_{\mathrm{in}} \\ b_{\mathrm{out}} \end{bmatrix} = \frac{i}{t} \begin{bmatrix} -1 & r \\ -r & r^2 + t^2 \end{bmatrix} \begin{bmatrix} a_{\mathrm{out}} \\ b_{\mathrm{in}} \end{bmatrix}, \tag{6}$$

and for the free-space component

$$\begin{bmatrix} a_{\mathrm{in}} \\ b_{\mathrm{out}} \end{bmatrix} = \begin{bmatrix} e^{iLk} & 0 \\ 0 & e^{-iLk} \end{bmatrix} \begin{bmatrix} a_{\mathrm{out}} \\ b_{\mathrm{in}} \end{bmatrix}. \tag{7}$$

Then we can define a matrix for each optical component as

$$M_{\mathrm{mirror}} = \frac{i}{t} \begin{bmatrix} -1 & r \\ -r & r^2 + t^2 \end{bmatrix} \quad \text{and} \quad M_{\mathrm{space}} = \begin{bmatrix} e^{iLk} & 0 \\ 0 & e^{-iLk} \end{bmatrix}. \tag{8}$$

This formalism is quite advantageous since now the input vector for the matrix equation of one optical component can be expressed as the output vector

of its alongside optical component. Then, to obtain the equations that govern a system one would just need to "chain" the matrix equations of each of the optical components of the system. To obtain a more clear view of how this method works let us take as an example the simple system of two optical components OC_1 and OC_2 in fig. 6.

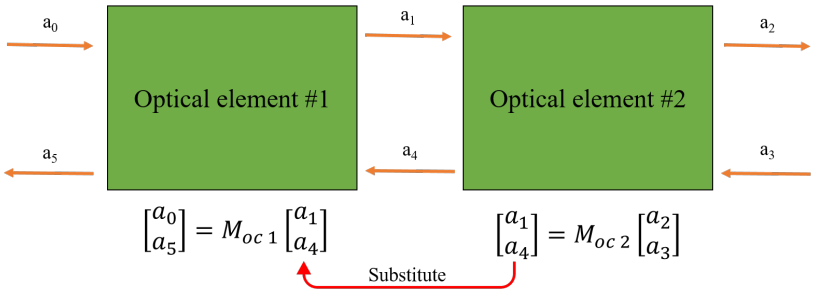

Figure 6: Example of a system with two optical components (mirrors, free space or both) used to explain the matrix formalism technique. The orange arrows are the incoming and outgoing light fields of the system, the green boxes are the optical components OC_1 and OC_2 and the matrix equations that appear under each optical component are their respective matrix equations.

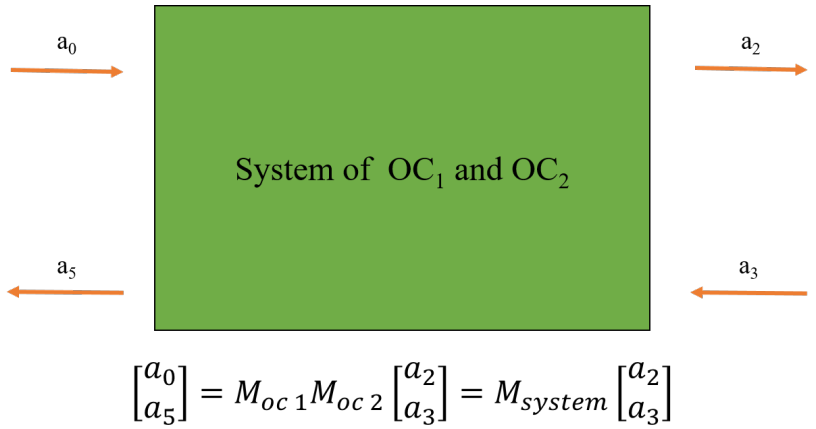

Figure 7: Depiction of how the two optical components in fig. 6 are chained together to produce one matrix equation for the whole system. With the matrix equation being dependent only of the light field vectors on the extremes of the system and the matrix of the system being $M_{\text{system}} = M_{\text{OC}_1} M_{\text{OC}_2}$

There, the two optical components can be mirrors, free space or both. The goal is to obtain a matrix equation, for the whole system, dependent only on the light fields that can be found at the extremes of the optical components.

This system as a whole has two incoming light fields a_0 and a_3 and two outgoing light fields a_2 and a_5 which are the ones at the extremes. The final equation should be in terms of just these four variables. In the middle of the two optical components one can find the light fields a_1 and a_4 which are shared by both optical components. This sharing then allows us to input the matrix equation of OC_2 into the matrix equation of OC_1 and this action is what we call the chaining. This is depicted in fig. 6. Then, after this substitution we can reduce our system of two optical components to just one optical component (refer to fig. 7) with a slightly more complicated matrix of the form

$$M_{\text{system}} = M_{\text{OC}_1} M_{\text{OC}_2}$$

We can add a third element to the system and then following the same procedure, chain its matrix equation to that of the system of already two components. This would yield a matrix equation for what would be a three component system. Chain N components and do the same procedure to obtain one matrix equation for an N optical component system.

3.3 TM cavity transmission and reflection functions

By executing the exact procedure showed in the previous section, we can obtain the three-mirror cavity matrix:

$$M_{\text{TM}} = M_{\text{mirror}_1} M_{\text{space}_1} M_{\text{mirror}_2} M_{\text{space}_2} M_{\text{mirror3}}$$

Where the matrices are the same as those of eq. (8) but they do not necessarily must have the same parameters. The exact analytical result can be obtained with the help of the symbolic manipulation package "SymPy":

$$M_{\text{TM}} = \begin{bmatrix} A & B \\ C & D \end{bmatrix}, \tag{9}$$

where

$$A = [(r_1 - r_2 e^{2iL_1k})r_3 - (r_1 r_2 - e^{2iL_1k})e^{2ikL_2}] \frac{ie^{-ik(L_1+L_2)}}{t_2 t_2 t_3},$$

$$B = [(r_1 r_2 - e^{2iL_1k})r_3 e^{2ikL_2} - (r_1 - r_2 e^{2iL_1k})] \frac{ie^{-ik(L_1+L_2)}}{t_2 t_2 t_3},$$

$$C = [(r_1 e^{2iL_1k} - r_2)e^{2ikL_2} - (r_1 r_2 e^{2iL_1k} - 1)r_3] \frac{ie^{-ik(L_1+L_2)}}{t_2 t_2 t_3},$$

$$D = [(r_1 r_2 e^{2iL_1k} - 1) - (r_1 e^{2iL_1k} - r_2)r_3 e^{2ikL_2}] \frac{ie^{-ik(L_1+L_2)}}{t_2 t_2 t_3}.$$

In these expressions, r_i and t_i are respectively the reflection and transmission coefficients of the i^{th} mirror, L_1 is the spacing between mirrors 1 and 2, and L_2 the spacing between mirror 2 and 3. Following the same scheme of fig. 7 our matrix equation would be

$$\begin{bmatrix} a_0 \\ a_6 \end{bmatrix} = M_{\text{TMsystem}} \begin{bmatrix} a_3 \\ 0 \end{bmatrix}, \tag{10}$$

then if we substitute eq. (9) into eq. (10) we can manipulate it to obtain the equations

$$t_{tm} = \frac{a_3}{a_0} = \frac{1}{A} = -\frac{it_1t_2t_3e^{ik(L_1+L_2)}}{(r_1 - r_2e^{2ikL_1})r_3 - (r_1r_2 - e^{2ikL_1})e^{2ikL_2}} \tag{11}$$

and

$$r_{tm} = \frac{a_6}{a_0} = \frac{C}{A} = \frac{(r_1e^{2ikL_1} - r_2)e^{2ikL_2} - (r_1r_2e^{2ikL_1} - 1)r_3}{(r_1 - r_2e^{2ikL_1})r_3 - (r_1r_2 - e^{2ikL_1})e^{2ikL_2}} \tag{12}$$

where t_{tm} is the transmission function and r_{tm} the reflection function of the of the TM cavity.

3.4 Equivalence between the effective mirror model and the TM cavity

Another way to derive equations (11) and (12) would be to use a convention in which the mirror component system of equations would be expressed as

$$\begin{cases} a_{\text{out}} = r'b_{\text{in}} + ta_{\text{in}} \\ b_{\text{out}} = ra_{\text{in}} + t'b_{\text{in}} \end{cases} \tag{13}$$

where this time, r, t and r', t' are the reflection and transmission coefficients of the left and right sides of the mirror. With the exception that any of the four coefficients can be complex but, their absolute value must still be between 0 and 1. Then this system would have a scattering matrix

$$S = \begin{bmatrix} t & r' \\ r & t' \end{bmatrix} \tag{14}$$

and to assure its unitarity, it is decided that

$$r' = \overline{r} \quad \text{and} \quad t' = -\overline{t}$$

where the line on top of r and t means the complex conjugate of the variable. Then, this new convention would cause the transmission and reflection functions of the FP cavity to transform into

$$t_{\text{FP}} = \frac{t_2t_1e^{-ikL}}{1 - r_1'r_2e^{-2ikL}} \tag{15}$$

$$r_{\text{FP}} = \frac{\overline{r_1'} - r_2e^{-2ikL}}{1 - r_1'r_2e^{-2ikL}} \tag{16}$$

.

Then, referring to the effective mirror scheme in fig. 5, the coefficients

$$t_{\text{eff}} = \frac{-it_1t_2e^{-iL_1k}}{1 - r_1r_2e^{-2iL_1k}} \tag{17}$$

$$r'_{\text{eff}} = \frac{r_2 - r_1e^{-2iL_1k}}{1 - r_1r_2e^{2iL_1k}} \tag{18}$$

can be assigned to the effective mirror and then by exchanging t_1 and r'_1 by t_{eff} and r'_{eff}, and t_2 and r_2 by t_3 and r_3 in eqs.(16) and (15) one would obtain

$$t_{\text{TM}} = \frac{t_{eff}t_3e^{-ikL_2}}{1 - r'_{eff}r_2e^{-2ikL_2}} \tag{19}$$

$$r_{\text{TM}} = \frac{\overline{r'_{eff}} - r_3e^{-2ikL_2}}{1 - r'_{eff}r_3e^{-2ikL_2}} \tag{20}$$

which in fact are the transmission and reflection coefficients of the TM cavity.

This interpretation gives us a much better intuition than the full formula (11) on the functioning of the three mirrors cavity. Indeed, the first sub-cavity of length L_1 can be thought of as an input mirror for the long cavity of length L_2. Furthermore, formula (17) shows that the transmission of this effective input mirror can be tuned in-situ by changing the length L_1 of the first sub-cavity.

3.5 Practical parameter tuning for the TM cavity mirrors

Not any value of T's and L's would be useful to make an FP cavity work and the same applies to the TM cavity. To make an FP cavity work (particularly near the high finesse approximation) T_1 and T_2 must be very small and at the same time $T_2 < T_1$. The same would apply to the effective mirror scheme in fig. 5, in that case it can be said that $|t_{\text{eff}}|^2 = T_{\text{eff}}$ and hence to achieve the high finesse approximation T_{eff} and T_3 will have to be very small and $T_3 < T_{\text{eff}}$. Then using these two variables and eq. (3) the BW for the TM cavity resonance peaks would be

$$BW_{\text{TM}} \approx \frac{c}{8\pi L_2}(T_{\text{eff}}+T_3) = \frac{c}{8\pi L_2}\left(\frac{T_1T_2}{1 - 2r_1r_2\cos(2L_1k) + (r_1r_2)^2} + T_3\right) \tag{21}$$

where now it is explicit that the bandwidth of the cavity will be dependent on L_1 and k. Then it is easy too see that for a given f_{res} the maximum value of the BW_{TM} will occur when T_{eff} gets maximized which occurs when the short cavity is in resonance. That is, the condition $2L_1k = 2N\pi$ is fulfilled and this implies that

$$L_1^{\max} = \frac{Nc}{2f_{\text{res}}} = N\frac{\lambda_{\text{res}}}{2}. \tag{22}$$

By the same analysis, the minimum value of BW_{TM} will occur when T_{eff} is minimized, which occurs when the short cavity is in anti-resonance and this happens when the condition $2L_1k = (2N+1)\pi$ is fulfilled and this implies that

$$L_1^{\min} = \left(N + \frac{1}{2}\right) \frac{c}{2f_{\text{res}}} = \left(N + \frac{1}{2}\right) \frac{\lambda_{\text{res}}}{2} \tag{23}$$

where N is an integer and $\lambda_{\text{res}} = c/f_{\text{res}}$. Then to tune the bandwidth of the cavity it would be as simple as to tune L_1 to any intermediate value between $L_1^{\max}$ and $L_1^{\min}$. The techniques that can be employed for the stabilization of such an optical system with a precision greatly exceeding 1 micron goes beyond the scope of this work.

To see the effects on the bandwidths of the peaks by varying L_1 an example was generated (fig. 8) by setting the wavelength of resonance to be $\lambda = 1094$nm. The parameters of the FP and TM cavities were set up as they appear in tables (1) and (2) respectively. These parameters were selected without any particular reason other than they managed to highlight the extreme changes that can be achieved in the bandwidths of the peaks by doing very small changes in L_1. In the graphs of fig. 8 there appears a comparison between an FP cavity of length L=2.735km, a TM cavity with cavity lengths of $L_1^{\max}$=547nm=$\lambda_{\text{res}}/2$ and L_2=2.735km and a TM cavity with lengths of $L_1^{\min}$=820.5nm=$1.5\lambda_{\text{res}}/2$ and L_2=2.735km. These graphs clearly show how the bandwidths of the peaks drastically changed caused by the manipulation of the L_1 parameter. In that same figure, the orange graph in the bottom show how the BW_{TM} of the peaks will depend on the parameter of L_1. It was generated by varying L_1 between the range of $[0.5L_1^{\max}, 1.5L_1^{\max}]$ at constant $k = \frac{2\pi f_{\text{res}}}{c}$ within equation (21). The red and green constant lines in the bottom of the figure shows the maximum and minimum achievable BW_{TM} values. Lastly, the blue constant line is the BW_{FP} of the comparative FP cavity which has no way of being changed. This graphs explicitly show the advantage of the TM cavity over the FP cavity.

FP cavity parameters

L [km]	2.735
T_1	0.2
T_2	0.005
BW [Hz]	894.082

Table 1: Parameters that describe the graph of the reflection function of the FP cavity in fig. (8). The last parameter was calculated by using the equation (3)

TM cavity parameters

$L_1^{\min}$ [nm]	$820.5 = \frac{1.5\lambda_{\text{res}}}{2}$
$L_1^{\max}$ [nm]	$547 = \frac{\lambda_{\text{res}}}{2}$
L_2 [km]	2.735
T_1	0.09
T_2	0.02
T_3	0.1
$BW_{\min}$ [Hz]	438.21
$BW_{\max}$ [Hz]	2971.21

Table 2: Parameters that describe the graphs of the reflection function of the TM cavity in fig. (8). The last two parameters are calculated by using the equation (21) and the corresponding $L_1^{\min}$ and $L_1^{\max}$.

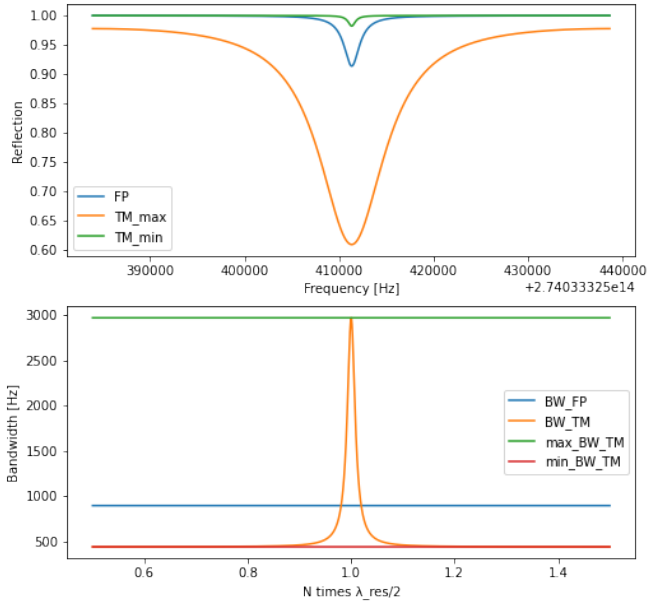

Figure 8: (Upper graphs) The blue line shows the reflection function of an FP cavity with the parameters that appear in table 1. The green line shows the reflection function of a TM cavity with the parameters that appear in table 2 and particularly with $L_1 = L_1^{\min}$. The same goes for the orange line except that this time $L_1 = L_1^{\max}$. (Bottom graphs) Blue constant line is the BW_{FP} where value can be found in table 1. The orange line is the BW_{TM} as a function of L_1 and with constant $k = \frac{2\pi f_{\text{res}}}{c}$. The green and red constant lines mark the max. and min. achievable values for BW_{TM}.

4 Conclusion

Currently, the state of the art to reduce the QN in the gravitational waves detection is to use FP cavities with a certain degree of phase squeezing but it doesn't have to be like that anymore as it has been shown in this report. It has been shown that there are two ways in which a TM cavity can have its equations derived. By using the matrix formalism or by re-interpreting the TM cavities as FP cavities with an effective mirror. This re-interpretation then gives permission to use the formulas of the FP cavities at the high finesse approximation and hence derive equation (21) and it is this equations that shows that TM cavities have the ability to tune their BWs. Ability which then allows for the control of the phase squeezing process and hence to be able to produce frequency dependent squeezed light. There are still other challenges ahead like the required stabilization system that would need to have a precision beyond 1 micron, which would be a whole other project on its own. Nonetheless, to have the theoretical framework for the TM cavity is to be already one step closer to its construction and deployment.

5 Acknowledgements

This project was supported in part by the NSF grants NSF PHY-1950830 and NSF PHY-1460803 and by the University of Florida physics department.

References

[1] Charlotte Bond, Daniel Brown, Andreas Freise, and Kenneth A Strain. Interferometer techniques for gravitational-wave detection. *Living reviews in relativity*, 19(1):1–217, 2016.

[2] S S Y Chua, B J J Slagmolen, D A Shaddock, and D E McClelland. Quantum squeezed light in gravitational-wave detectors. *Classical and Quantum Gravity*, 31(18):183001, sep 2014.